Development of Electronic Control Emergency Generator Engine for Data Center

SOTA WATANABE[*1] HISAO OGAWA[*2]
TARO TAMURA[*3] YUSUKE IMAMORI[*4]
KENGO TANAKA[*4] SEIJI TSURUOKA[*5]

In order to respond the increase in required power output of emergency generator engines for data centers and semiconductor factories, Mitsubishi Heavy Industries Engine & Turbocharger, Ltd. (MHIET) has developed an electronically controlled emergency generator engine that is based on our currently marketed S16R2 and has a 10% higher power output while maintaining the same footprint. This engine has achieved improved dynamic performance and emissions performance as well as higher output by being equipped with a common-rail electronically controlled fuel injection system developed in-house. The performance and durability tests of the engine alone have been completed so far. We plan to bring this engine to the market after completing the performance verification of a generating set consisting of the engine coupled with a generator.

1. Introduction

In recent years, the demand for emergency power generation for data centers and semiconductor factories has been increasing, and the need for higher output in limited space has increased single unit outputs. Even with the trend toward carbon neutrality, the need for emergency generator diesel engines remains high due to their short operating time, which means low carbon dioxide emissions.

To meet the above-mentioned market needs, MHIET has developed a new electronically controlled emergency generator engine, S16R2-PTAWT-CR. This engine is based on our currently marketed S16R2 and has a 10% higher power output while maintaining the same footprint by improving the brake mean effective pressure (BMEP), which represents the amount of work per cycle and unit displacement.

Chapter 2 introduces the main specifications of the S16R2-PTAWT-CR and technologies applied thereto. The engine is equipped with turbochargers and an air cooler to deal with the increased power output. In addition, in response to a 10% increase in the BMEP, the maximum in-cylinder pressure (Pmax) was increased by approximately 10%, and the reliability of each component was evaluated using a large-scale 3D finite element method (FEM) to optimize the materials and shapes of the cylinder head, cylinder liner, and crankcase. Furthermore, due to the employment of a common-rail electronically controlled fuel injection system (CRS) developed in-house, not only higher output, but also improved dynamic performance and emissions performance were achieved.

Chapters 3 and 4 introduce a desk study and actual engine verification of the engine performance, such as rated output performance and dynamic performance, of S16R2-PTAWT-CR,

*1 Project Manager, Engine Technology Development Department, Engine & Energy Division, Mitsubishi Heavy Industries Engine & Turbocharger, Ltd.
*2 Manager, Engine Technology Development Department, Engine & Energy Division, Mitsubishi Heavy Industries Engine & Turbocharger, Ltd.
*3 Engine Technology Development Department, Engine & Energy Division, Mitsubishi Heavy Industries Engine & Turbocharger, Ltd.
*4 Chief Staff Researcher, Combustion Research Department, Research & Innovation Center, Mitsubishi Heavy Industries, Ltd.
*5 Chief Staff Researcher, Strength Research Department, Research & Innovation Center, Mitsubishi Heavy Industries, Ltd.

to which these technologies were applied.

2. Overview of S16R2-PTAWT-CR development

Table 1 shows the main specifications of the S16R2-PTAWT-CR. The output was increased by 10% from 2,750 kVA Stand-by to 3,000 kVA Stand-by compared to the existing model when the cylinder bore, stroke, rated speed, and number of cylinders were the same. As a result, the BMEP was increased by 0.2 MPa.

Table 1 Main specifications of S16R2-PTAWT-CR

		Existing model S16R2-PTAW2-S	Developed model S16R2-PTAWT-CR
Cylinder bore	mm	170	←
Stroke	mm	220	←
Rated speed	min^{-1}	1,500	←
Number of cylinders	—	16	←
Rated output	kVA Stand-by	2,750	3,000
BMEP	MPa	2.4	2.6
Fuel injection system	—	Mechanical fuel injection system	Common-rail electronically controlled fuel injection system

Figure 1 shows an external view of the S16R2-PTAWT-CR. Major changes from the existing model S16R2 include intake system components for higher output, structural components such as cylinder head, cylinder liner, and crankcase for higher BMEP, and fuel injection system components, electronic control components, and pistons for the application of CRS. These applied technologies are described below.

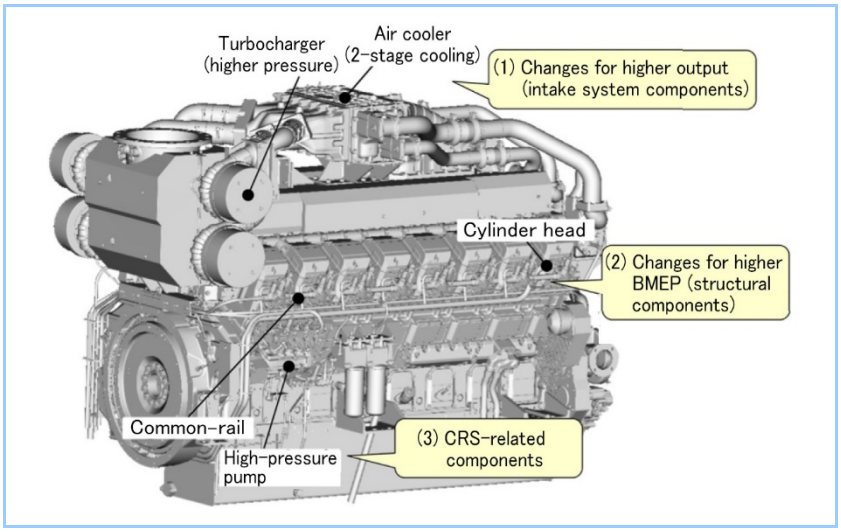

Figure 1 Engine external view

2.1 Changes in intake system components for higher output

In order to maintain the excess air ratio for higher output, turbochargers with a high-pressure ratio were applied. Since the increase in the intake air volume and pressure ratio associated with higher output increased the cooling water heat exchange amount in the air cooler, a two-stage air cooler was used. **Figure 2** shows the cooling water system diagram. While the high- and low-temperature water systems were separated for the water jacket and air cooler in the existing model, the S16R2-PTAWT-CR is equipped with the two-stage air cooler and, the high-temperature water bears part of the heat exchange amount in the air cooler, which causes the reduction of the heat exchange amount of the low-temperature water. By reducing the heat exchange amount of low-temperature water, which determines the size of the radiator, the size of the radiator could be reduced compared to the existing model. Although the size of the air cooler has increased with the adoption of the two-stage air cooler, the engine layout was designed so that it can fit into a high-cube container for transportation.

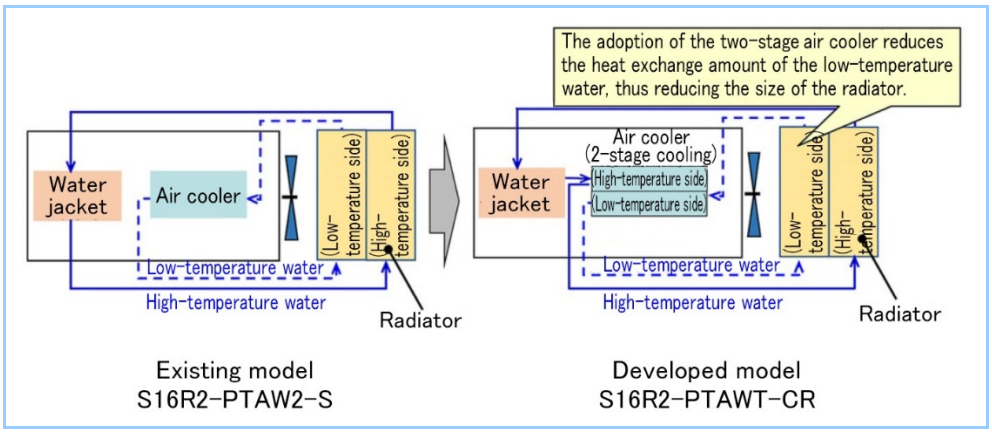

Figure 2 Cooling water system diagram

2.2 Reliability evaluation utilizing FEM and CFD

Since the Pmax was increased by approximately 10% in response to the 10% increase in the BMEP, stress and deformation calculations with respect to this higher BMEP and higher Pmax were performed using a large-scale 3D FEM to evaluate the reliability of each component. This section introduces the reliability evaluation of the cylinder head, cylinder liner, and crankcase. **Figure 3** shows the overall analysis model. To reduce the analysis load, the 3.5 cylinders shown in the figure were modeled. The analysis code was Adventure cluster ver. 2018, and the model size included 9,517,210 nodes and 7,448,850 elements.

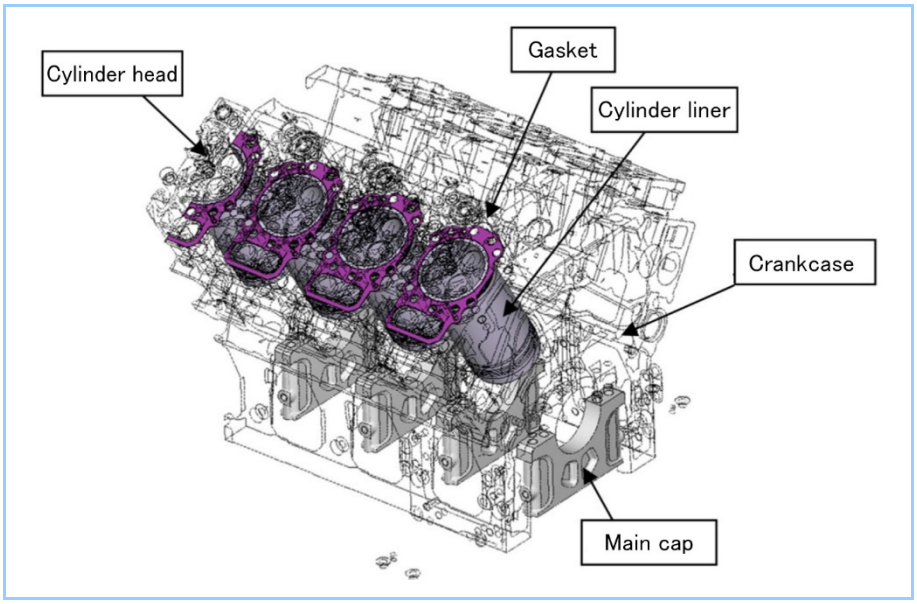

Figure 3 3D model used for analysis

In the modeling, nonlinearities such as "contact between the cylinder head bolts, cylinder head, gasket, cylinder liner, crankcase, and other parts," "elasto-plastic properties of the gasket material," and "temperature dependence of each physical property" were taken into account to improve the reproducibility and evaluation accuracy of actual phenomena. In addition, analysis of the cylinder head was also performed for different materials.

During engine operation, there are thermal and pressure loads due to the combustion of fuel in the cylinder. These loads change with the engine power output. Stress and deformation calculations were performed with these loads as FEM calculation conditions. We performed calculations with eight load steps to simulate the power output pattern of the actual engine. Thermal conditions were derived from computational fluid dynamics (CFD) analysis for the combustion chamber side and the cooling water channel side, and were added to the FEM analysis described above.

Based on the calculation result, we derived the stress and deformation of each component, and conducted fatigue evaluation and gasket sealing evaluation. For the fatigue evaluation, we

factored in the stress values for each of the eight load steps described above and used the combination that would maximize the stress amplitude. In addition, we adopted not an evaluation method based on the surface stress only, but a more accurate evaluation method considering the stress distribution from the surface to the inside of the wall thickness.

Figure 4 shows an example of high-cycle fatigue safety factor distribution on the cooling surface side of the cylinder head. Based on this examination, we optimized the materials to ensure reliability. The same evaluation was also conducted for the cylinder liner and crankcase. Especially for the upper part of the cylinder liner, the shape was optimized to maximize the safety factor. The surface pressure was evaluated at each load step, and the sealing performance of the gaskets was also evaluated.

We conducted reliability evaluations using FEM/CFD and then performed durability tests on actual engines. It was verified that each component had sufficient reliability.

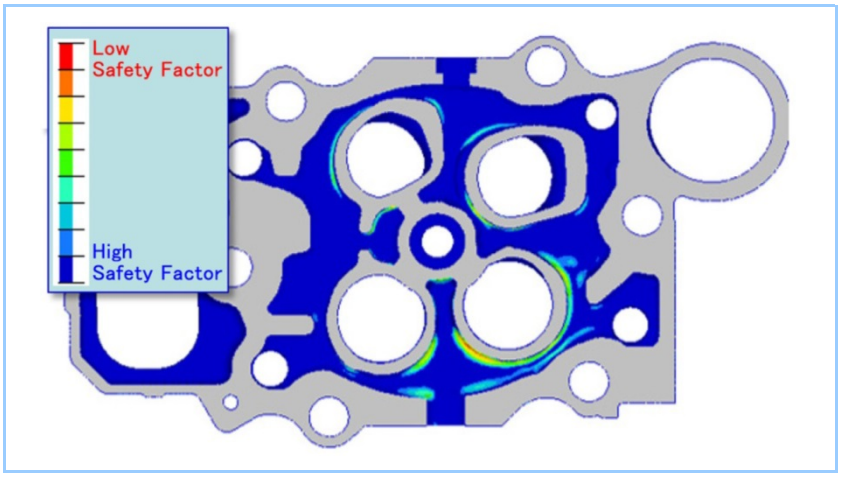

Figure 4 Example of high-cycle fatigue safety factor distribution

2.3 Development of common-rail electronically controlled fuel injection system

Up to now, our mainstay SR diesel engines have responded to customer needs over the years through improvements to the internal component parts of the mechanical injection pump, which were designed in-house for the fuel injection system. However, in this development of the S16R2-PTAWT-CR, we newly developed a common-rail electronically controlled fuel injection system with the highest degree of freedom in injection control, in order to achieve the development goals, such as higher output, better load response, and improved emissions performance. This section introduces the key points in the development of this system.

(1) System design

Figure 5 shows the configuration of the common-rail electronically controlled fuel injection system. This system controls the discharge rate of the high-pressure pump with respect to the amount of fuel discharged from the injectors, and the fuel is injected by hydraulically driving the injectors with a solenoid valve while maintaining a constant common-rail internal pressure as injection energy. Therefore, hydraulic control design is an important elemental technology for both the high-pressure pump and injectors. In designing this system, as shown in **Figure 6**, we improved the accuracy of the one-dimensional hydraulic analysis model so that the actual injection rate error of the injector, the final output, would be within 8%. We used the model to determine the target injection performance and design parameters for component strength and seal design that should be ensured under fluctuating hydraulic pressure conditions.

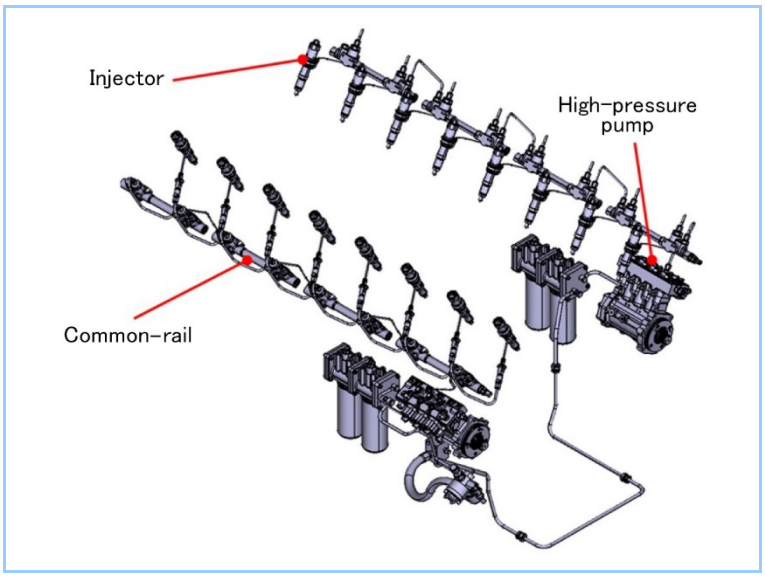

Figure 5 Configuration of common-rail electronically controlled fuel injection system

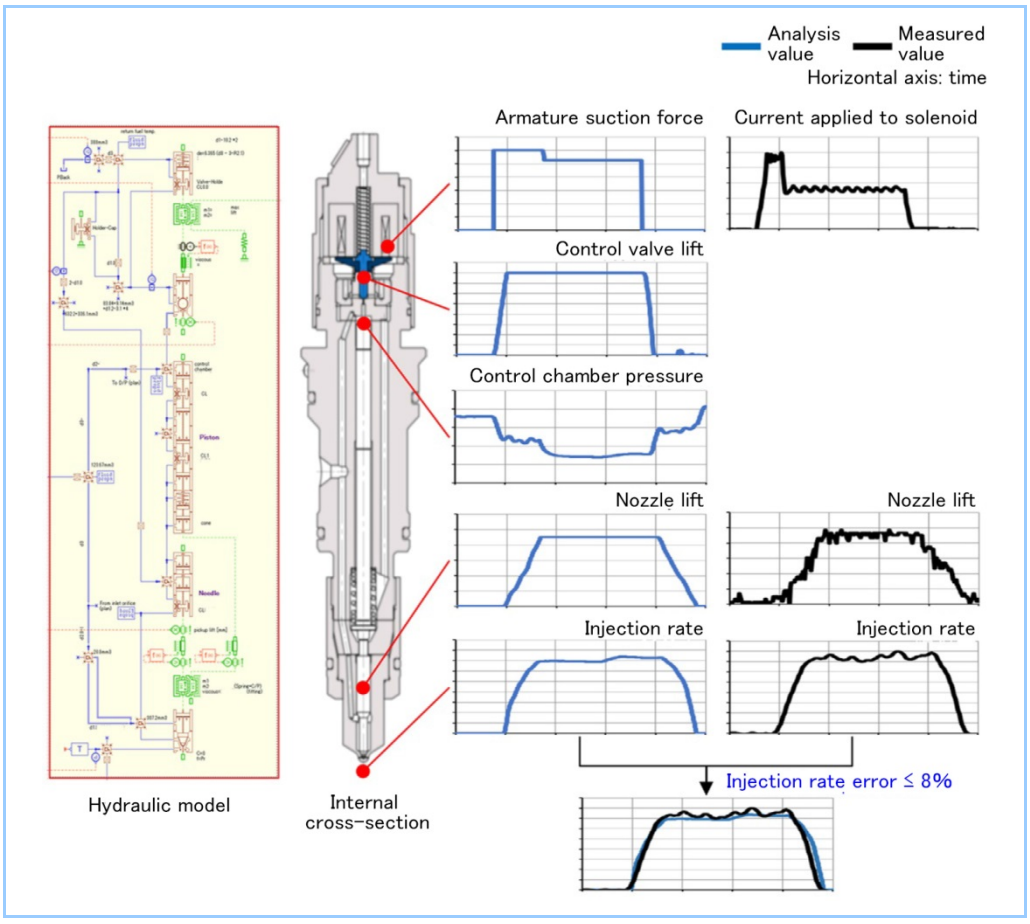

Figure 6 Example of efforts to improve accuracy of hydraulic analysis (injector)

(2) High-pressure injection technology

To improve the combustion efficiency of an engine, it is desirable to promote the atomization of fuel spray into the cylinder. For this reason, the system was designed to increase the fuel injection pressure by approximately 50% or more compared to the existing model S16R2. On the other hand, since the basic housing shape on the engine side follows the conventional product, the injector and high-pressure pump were designed to fit within the outline of the conventional injection system. **Figure 7** shows an example of such a structure. In order to alleviate stress concentration when high pressure is applied in the fuel passage, parallel nozzle ports were adopted for the injectors, and an offset cross passage structure was adopted for the high-pressure pump.

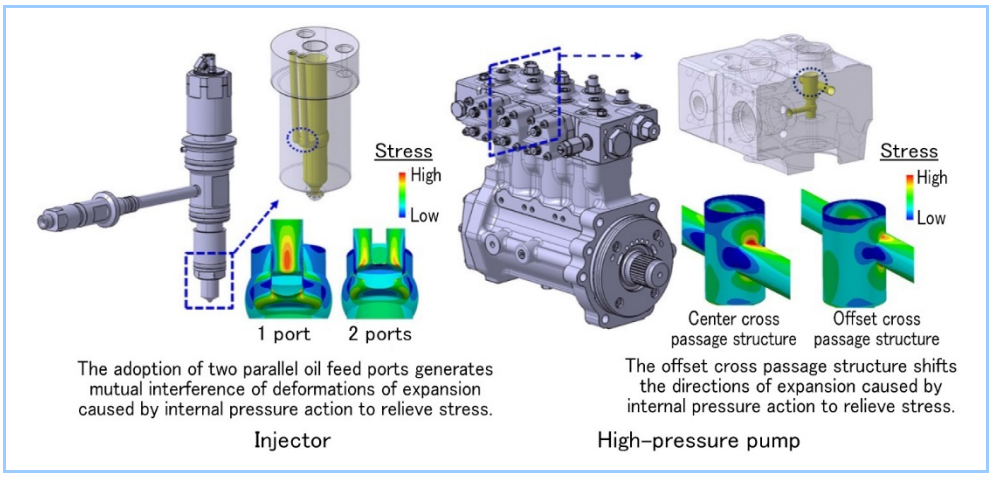

Figure 7 Examples of higher-pressure structure

(3) Technology to stabilize fuel injection of injectors

Figure 8 shows a structural of the injector solenoid valve. In the open/close operation of an injector solenoid valve, the bouncing of the valve at the time of seating greatly affects the change in injection volume before and after the bouncing. Especially for minute injection volumes, it causes a deterioration in controllability. In order to reduce the bouncing, the valve body was made approximately 50% lighter than the initial prototype structure by placing the valve closing spring inside the solenoid, and the valve body separates into two bodies when seated to reduce inertial mass.

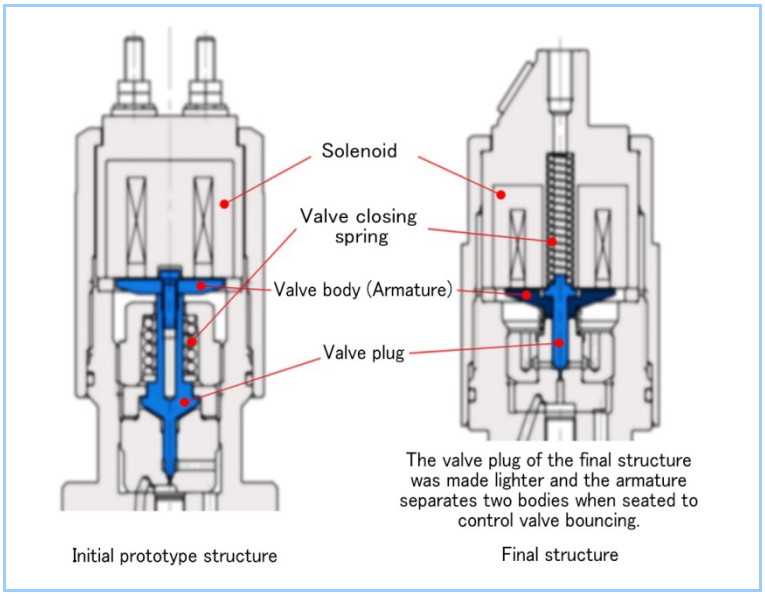

Figure 8 Structure of solenoid valve

(4) Technology to suppress variation in individual injector injection volume

The higher-pressure injection results in larger individual differences in injection volume for the same injection period, which leads to variations in the exhaust temperature and maximum pressure in each cylinder. So, the difference needs to be suppressed as much as possible in terms of reliability of the engine itself. Therefore, as shown in **Figure 9**, we incorporated technology to control the injection flow rate at the nozzle of each injector to ±1% using abrasive polishing technology and to suppress the variation of injection volume by electrically correcting the injection operation period of the injector by a controller.

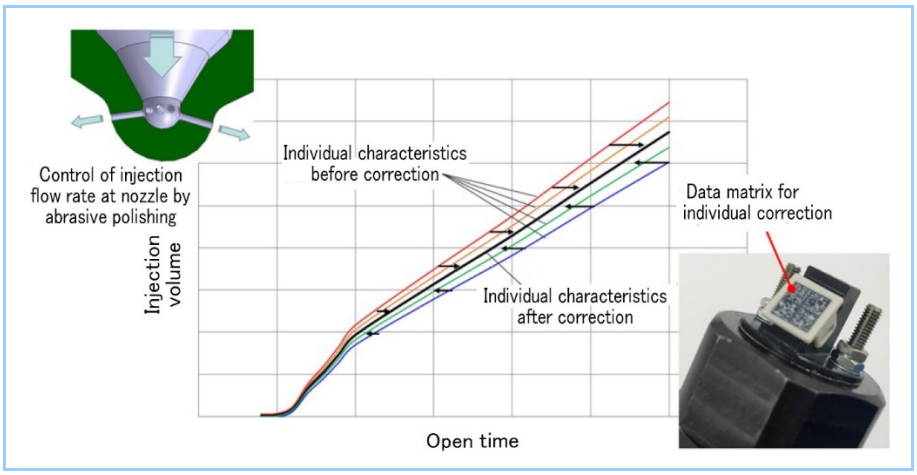

Figure 9 Technology to suppress variation of injection volume of individual injectors

3. Examination of engine performance

3.1 Simulation of rated output performance

In order to improve the power output by 10% compared to the existing model S16R2, the engine performance simulation code (GT-Power) was used to optimize engine specifications that can suppress the exhaust gas temperature and maximum in-cylinder pressure, which are the main limiting conditions. **Figure 10** shows the results of simulations using the intake valve closing timing, turbine nozzle area and fuel injection timing as parameters. When the intake valve is closed earlier, compared to the case it is closed later, an increase in turbocharger speed with an increase in exhaust gas temperature results in the same excess air ratio, but the trade-off relationship between the maximum in-cylinder pressure and exhaust gas temperature worsens. On the other hand, when the turbine nozzle area is reduced, the trade-off relationship between the maximum in-cylinder pressure and exhaust temperature improves due to the increase in the excess air ratio, and the exhaust temperature is expected to decrease by 7 K to 10 K at the same maximum in-cylinder pressure, so we selected this specification.

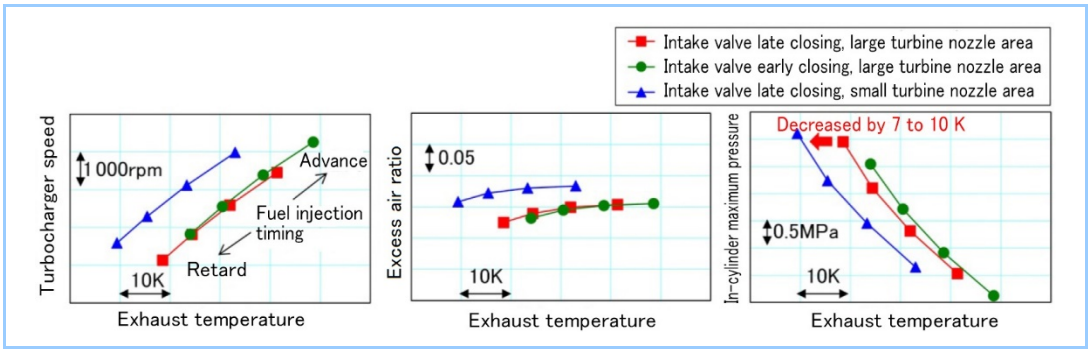

Figure 10 Result of engine performance simulation

Since there was concern that the increased power output would increase the heat load on the combustion chamber structural components, we performed combustion CFD with the piston shape and nozzle specifications as parameters to optimize the flame distribution. **Figure 11** shows the analysis result of the temperature distribution in the combustion chamber after the optimization. The flame is dispersed over a wide area in the directions of the piston surface and liner, which is expected to suppress the local temperature rise of the structural components.

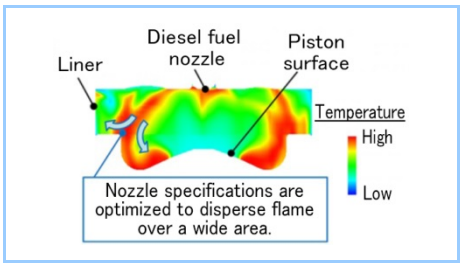

Figure 11 Result of combustion CFD

3.2 Simulation of dynamic performance

For newly installing the CRS, the dynamic characteristics such as load acceptance performance as a generating set were examined by simulation. **Figure 12** shows the simulation model. For the engine itself, the GT-Power model described in the previous section was used, linking it with the fuel injection control by the engine controller and MATLAB/Simulink models for the generator control, so that the dynamic characteristics with respect to the detailed specifications of the engine itself can be evaluated. **Figure 13** shows an example of the analysis result. By reducing the turbine nozzle area of the turbocharger, the frequency recovery time when the load is applied to the generating set was reduced. Using this simulation, the specifications of the engine itself and the generator were optimized.

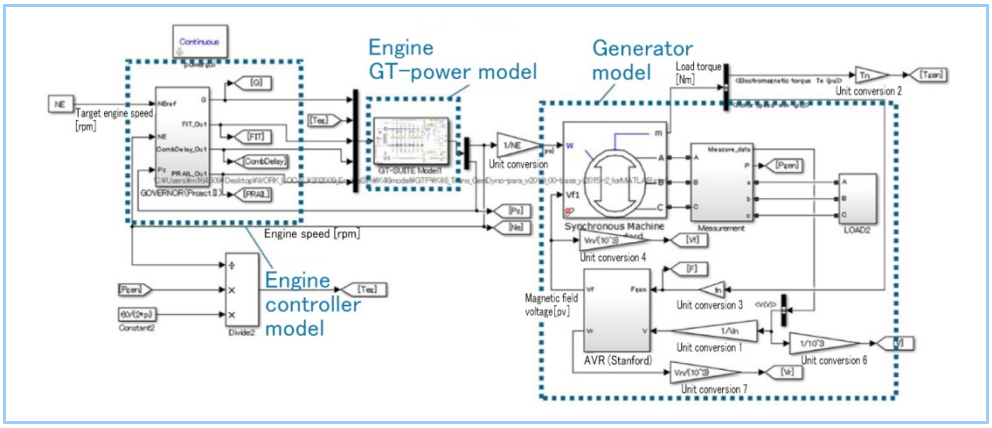

Figure 12 Generator set simulation model

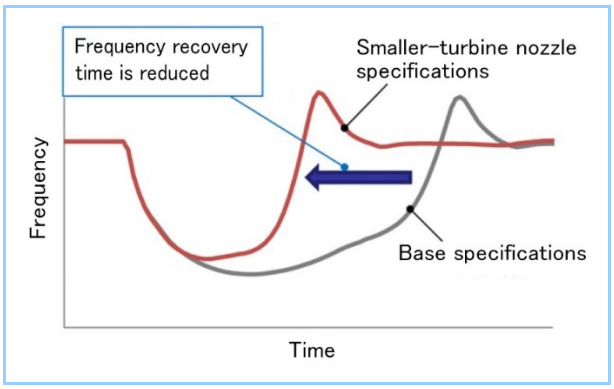

Figure 13 Example of generator set load acceptance performance analysis result

4. Result of performance test on actual engine

We utilized various simulations to test the performance of the selected engine specifications. This chapter presents the main performance characteristics of the S16R2-PTAWT-CR in comparison with our currently marketed S16R2.

4.1 Rated output performance and emissions performance

Figure 14 shows the main engine performance at rated output and **Figure 15** shows the combustion performance. For the S16R2-PTAWT-CR, we took advantage of the high flexibility in setting the fuel injection, which is one of the characteristics of the CRS, to select the appropriate

fuel injection pressure and timing according to the combustion system specifications (pistons, etc.) to optimize the fuel-air mixture inside the cylinder and combustion. As a result, the rated output was improved by 10% while maintaining the same specific fuel consumption as existing models by improving the degree of constant volume while maintaining the same level of cooling loss and combustion efficiency as existing models. In terms of emissions performance, by optimizing the fuel injection pattern at each point of the D2 mode, a significant reduction in the emissions mode value (NOx + HC: reduced by 36%) was achieved, which confirmed the potential to meet the EPA (Environmental Protection Agency) Tier 2 regulations.

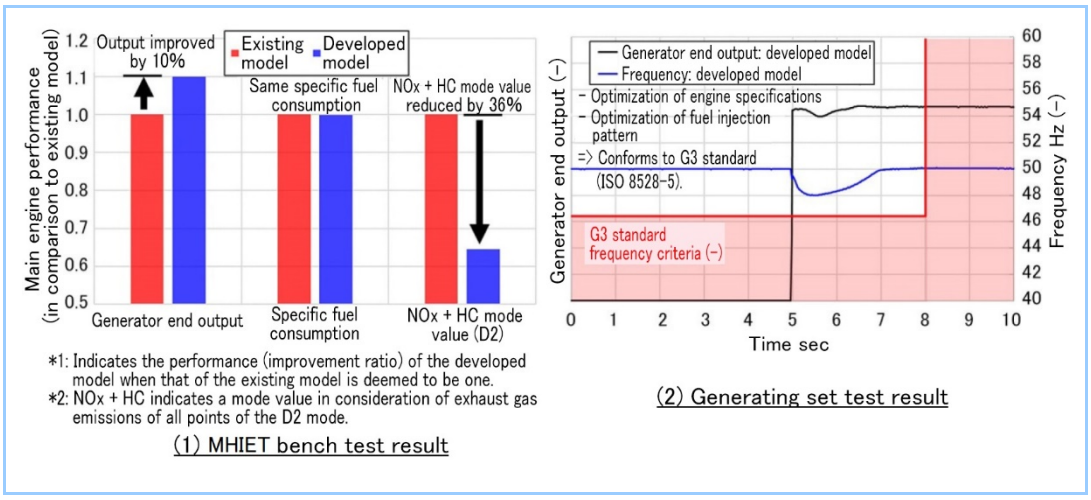

Figure 14 Main engine performance

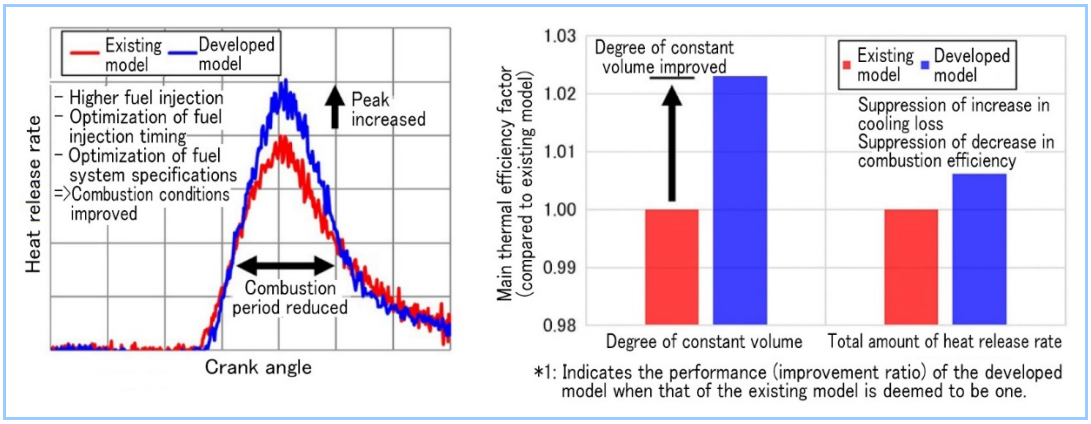

Figure 15 Combustion conditions (rated output: in-house bench test result)

4.2 Dynamic performance

Figure 14 shows the dynamic performance of a generating set consisting of the S16R2-PTAWT-CR coupled with a generator as a representative example of the dynamic performance. The dynamic performance conforms to the G3 standard (ISO 8528-5) in terms of stand-by output, and also achieves first step 100% load. As with the rated output performance and emissions performance, we took advantage of the CRS's high flexibility in fuel injection setting to achieve the target dynamic performance by optimizing the fuel injection pattern according to the engine combustion performance of each load condition based on the simulation results and the actual engine test results.

We plan to further improve the engine performance in the future by improving the combustion system specifications, such as pistons and injectors, and fuel injection patterns.

5. Conclusion

In order to address the increasing power output of emergency generator engines for data centers and semiconductor factories, we have developed the S16R2-PTAWT-CR electronically controlled emergency generator engine equipped with CRS.

This engine achieves a 10% increase in power output and a significant reduction in the emissions mode value while maintaining a specific fuel consumption equivalent to that of existing

models. The engine's dynamic performance conforms to the G3 standard (ISO 8528-5) in terms of stand-by output, and first step 100% load has also been achieved. In addition, sufficient reliability has also been confirmed through large-scale 3D FEM/CFD analysis and durability engine tests on actual equipment.

We plan to bring this engine to the market after completing the performance verification of a generating set consisting of the engine coupled with a generator.